



Short communication

High-rate discharge properties of nickel hydroxide/carbon composite as positive electrode for Ni/MH batteries

W.K. Zhang^a, X.H. Xia^a, H. Huang^{a,*}, Y.P. Gan^a, J.B. Wu^b, J.P. Tu^b^a College of Chemical Engineering and Materials Science, Zhejiang University of Technology, Hangzhou 310032, China^b Department of Materials Science and Engineering, Zhejiang University, Hangzhou 310027, China

ARTICLE INFO

Article history:

Received 30 November 2007

Received in revised form 1 March 2008

Accepted 12 March 2008

Available online 21 March 2008

Keywords:

Ni/MH batteries

Nickel hydroxide

Carbon black

High-rate discharge

Positive electrode

ABSTRACT

A chemical co-precipitation method was attempted to synthesize nickel hydroxide/carbon composite material for high-power Ni/MH batteries. The XRD analysis showed that there were a large amount of defects among the crystal lattice of the Ni(OH)₂/C composite, and the SEM investigation revealed that the as-synthesized spherical particles were composed of hundreds of nanometer crystals with a unique three-dimensional petal shape. Compared with pure Ni(OH)₂, the Ni(OH)₂/C composite showed improved electrochemical properties such as superior cycling stability, higher discharge capacity and higher mean voltage of discharge under high-rate discharge conditions, the discharge capacity and the mean discharge voltage of the Ni(OH)₂/C composite were about 281 mAh g⁻¹ and 0.303 V (vs. Hg/HgO) at 1 C-rate, 273 mAh g⁻¹ and 0.296 V at 5 C-rate, 250 mAh g⁻¹ and 0.292 V at 10 C-rate, respectively. The cyclic voltammetry (CV) tests showed that the Ni(OH)₂/C composite exhibited good electrochemical reversibility and the formation of γ-NiOOH during the charge–discharge processes was prevented. The existence of carbon in the Ni(OH)₂/C composite contributed great effect on the improvement of high-rate discharge performance.

© 2008 Elsevier B.V. All rights reserved.

1. Introduction

Nickel/metal hydride (Ni/MH) batteries are considered to be one of the most promising choices for electric vehicle (EV) and hydride electric vehicle (HEV) applications due to high power and low cost [1]. Active electrode materials for high-power batteries should possess high-proton diffusion coefficients and high-electronic conductivity. Nickel hydroxide (β-Ni(OH)₂), the active material of the positive electrode of Ni/MH battery, is a kind of p-type semiconductor and its poor electronic conductivity handicaps the high-rate dischargeability of Ni/MH batteries [2,3].

So far, many attempts have been made to improve the electronic conductivity of Ni(OH)₂ [4–8]. The commonly used approach is to add cobalt additive (CoO, Co(OH)₂, etc.) directly to the positive electrode, which will form a CoOOH conductive film on the spherical Ni(OH)₂ surface. It is believed that the presence of cobalt bestows many beneficial effects such as increased oxygen evolution overpotential, reduced electric resistance, increased utilization of the active material and improved electrochemical reversibility [9,10]. However, this physical mixture of Ni(OH)₂ and additives is not effective to reduce the inner resistance of the particles.

The high-rate dischargeability of the positive electrode cannot be improved satisfactorily. An alternative approach is the addition of cobalt to the lattice of Ni(OH)₂ by chemical co-precipitation [11,12]. It was experimentally found that nickel species accumulate at the hydroxide/electrolyte interface during discharge and these species are insulated, they have high-interface resistance and prevent discharge of the crystallite core [13]. Moreover, there is still some controversy whether the electronic conductivity is increased through the addition of cobalt to the inner crystal of Ni(OH)₂. Corrigan has reported that there was no evidence that any of the co-precipitated metal ions provided dopant states which increased the electronic conductivity [14].

Highly conductive carbon black, known for its highly accessible surface, low resistance and good chemical stability, is considered as conductive agent in batteries [15–17]. Nevertheless, the main utilization way is still physical mixture of active material and carbon. There are two disadvantages about the physical mixture process: (1) carbon black has low density and large volume, so its existence will decrease the load of Ni(OH)₂ active material in the porous nickel substrate and (2) the utilization efficiency of carbon black is relatively low because it is difficult to achieve sufficient contact between the conductor and active material. In this study, a new Ni(OH)₂/C composite was synthesized by a co-precipitation method. It is anticipated that carbon black can be mixed homogeneously with Ni(OH)₂ particles during the co-precipitation process.

* Corresponding author. Tel.: +86 571 8832 0873; fax: +86 571 8832 0394.
E-mail address: hhui@zjut.edu.cn (H. Huang).

The high-rate dischargeability of the electrode can be modified by coexisting of carbon black within the $\text{Ni}(\text{OH})_2$ particles.

2. Experimental

2.1. Synthesis of $\text{Ni}(\text{OH})_2/\text{C}$ composite

Highly conductive carbon black used in this study was obtained from Shenzhen Yongkang Technology Company of China. The specific surface area is about $1100 \text{ m}^2 \text{ g}^{-1}$ and the particle size is about 30–40 nm. The resistivity is about 0.2–0.6 $\Omega \text{ cm}$. The $\text{Ni}(\text{OH})_2/\text{C}$ composite were fabricated by a co-precipitation method. NaOH aqueous solution (4 mol L^{-1}), NH_3 aqueous solution (2 mol L^{-1}) and a mixed aqueous solution of NiSO_4 , CoSO_4 and ZnSO_4 (molar ratio of Ni:Co:Zn is 100:1.5:3) were added into an ethanol solution with carbon black (CB) in the given ratio (weight ratio of $\text{Ni}(\text{OH})_2:\text{CB}$ is 100:1). The concentration of NiSO_4 aqueous solution was 2.0 mol L^{-1} . In order to improve the dispersion of carbon black, the ethanol solution was treated by ultrasonic for 30 min before addition. The precipitation reaction was carried out at 55°C with homogeneous stirring at pH value 10.5 for 18 h. The precipitate was then washed with distilled water, filtered and dried at 80°C for 24 h. For comparison, pure $\text{Ni}(\text{OH})_2$ was also synthesized by the same co-precipitation process without the addition of carbon black. The same reagents as above were used.

The as-prepared powders were characterized by X-ray diffraction (XRD, Philips PC-APD X-ray diffractometer with Cu K α radiation) and scanning electron microscope (SEM, HITACHI S-4700 II). The carbon content of $\text{Ni}(\text{OH})_2/\text{C}$ sample was measured by Vario EL III elemental analyzers.

2.2. Preparation of positive electrode and electrochemical tests

The as-synthesized $\text{Ni}(\text{OH})_2/\text{C}$ composite or pure $\text{Ni}(\text{OH})_2$ as active material was mixed with 4 wt.% CoO and a milling procedure was needed to ensure the uniformity of the mixture. Followed by an addition of proper amount of binders (PTFE and CMC) and distilled water, a homogeneous slurry with adequate rheological properties was made. The slurry was filled into a foam nickel substrate (1.5-mm thick) and dried at 75°C for 2 h. Afterwards, the positive electrode was rolled to a thickness of 0.72 mm.

The as-fabricated positive electrode, together with a nickel mesh counter electrode and an Hg/HgO reference electrode was tested in a three-compartment system. The electrolyte was 6 mol L^{-1} KOH solution. The galvanostatic charge–discharge tests were conducted with a BS-9390 battery program-control test system at room temperature ($25 \pm 1^\circ \text{C}$). For activation, the electrodes were charged at 0.1 C-rate for 15 h and discharged at 0.2 C-rate to a limited voltage of 0.1 V (vs. Hg/HgO), and then charged for 7.5 h and discharged to 0.1 V at 0.2 C-rate for four times. In the subsequent charge–discharge cycling tests, the electrodes were charged at 1 C-rate for 1.2 h and discharged at 1, 5, 10 C-rate. The corresponding cut-off voltages were set as 0.1, 0, 0 V (vs. Hg/HgO). Cyclic voltammetric (CV) measurements were performed after activation using a CHI660B electrochemical workshop with a scanning rate of 0.1 mV s^{-1} .

3. Results and discussion

3.1. Microstructure and morphology

The XRD patterns of the as-prepared $\text{Ni}(\text{OH})_2$ samples are shown in Fig. 1. It can be seen that the diffraction peaks of both samples are indexed as the hexagonal phase of typical $\beta\text{-Ni}(\text{OH})_2$ (JCPDS 14-0117). The diffraction peaks of the $\text{Ni}(\text{OH})_2/\text{C}$ composite are

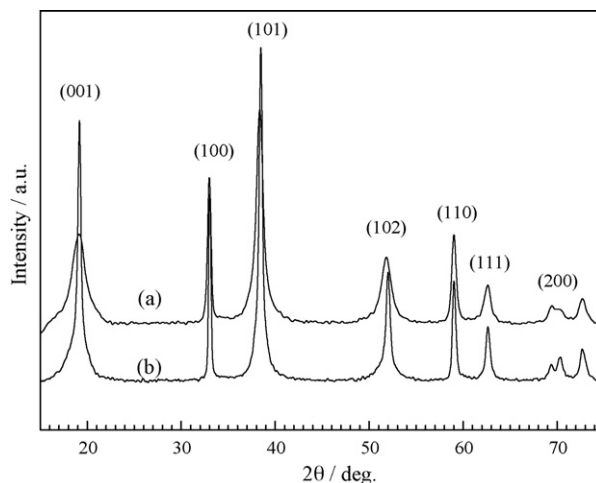


Fig. 1. XRD patterns of the $\text{Ni}(\text{OH})_2$ powders: (a) $\text{Ni}(\text{OH})_2/\text{C}$ composite and (b) pure $\text{Ni}(\text{OH})_2$.

noticeably broadened as compared to those of pure $\text{Ni}(\text{OH})_2$, indicating the poor crystallinity or smaller crystalline size of $\text{Ni}(\text{OH})_2/\text{C}$ material. The (001) diffraction line is the most intense in pattern (b), while the (101) diffraction line is the most intense in pattern (a), indicating that the crystal of $\text{Ni}(\text{OH})_2/\text{C}$ grows mainly in the direction perpendicular to the (101) plane to form sheet structure.

The reasons for broadening of the (001) reflection are due to small particle size, increased disorderliness on account of the existence of stack faults, and the presence of other polymorphic modifications as interstratified phases [18,19], those are identified to be crystal defects. Therefore, the abnormal width of (001) and (101) reflections are caused by the existence of defects in the material. A large amount of structural defects are distributed among the volume of the crystal lattice of the as-prepared $\text{Ni}(\text{OH})_2/\text{C}$ composite. It has been reported that $\text{Ni}(\text{OH})_2$ particles with more crystal defects possess higher proton diffusion coefficients and have better electrochemical performance [20,21].

Fig. 2 illustrates the morphology of the $\text{Ni}(\text{OH})_2$ samples. As shown in Fig. 2, the synthesized $\text{Ni}(\text{OH})_2/\text{C}$ and $\text{Ni}(\text{OH})_2$ particles are spherical with sizes of about $10 \mu\text{m}$ in diameter. Moreover, the spherical particles are composed of hundreds of nanometer crystals with a unique three-dimensional petal shape owing large surface area and inner space. As compared with pure $\text{Ni}(\text{OH})_2$, the microstructure of the $\text{Ni}(\text{OH})_2/\text{C}$ composite becomes looser. It may facilitate electrolyte soaking into particles, the insertion and de-insertion of proton during the charge–discharge process and hence may improve the electrochemical performance of $\text{Ni}(\text{OH})_2$ material. The carbon content in the $\text{Ni}(\text{OH})_2/\text{C}$ composite is about 1.21 wt.%.

3.2. Cycle stability under high-rate discharge conditions

To evaluate the effect of carbon introduced by the co-precipitation process on the electrochemical performance of the $\text{Ni}(\text{OH})_2/\text{C}$ composite, the discharge capacities of the $\text{Ni}(\text{OH})_2/\text{C}$ samples with different carbon content were measured at 1 C-rate after activation. Fig. 3 shows the charge–discharge curves of the $\text{Ni}(\text{OH})_2/\text{C}$ samples with different carbon content. It is found that the optimum carbon content of $\text{Ni}(\text{OH})_2/\text{C}$ composite is about 1.21 wt.% to obtain the highest discharge capacity (287.3 mAh g^{-1}), which is close to the theoretical capacity of $\text{Ni}(\text{OH})_2$ ($Q_{\text{theory}} = 289 \text{ mAh g}^{-1}$). The high-rate dischargeability of the $\text{Ni}(\text{OH})_2/\text{C}$ composite with the content of about 1.21 wt.% was investigated in detail hereafter.

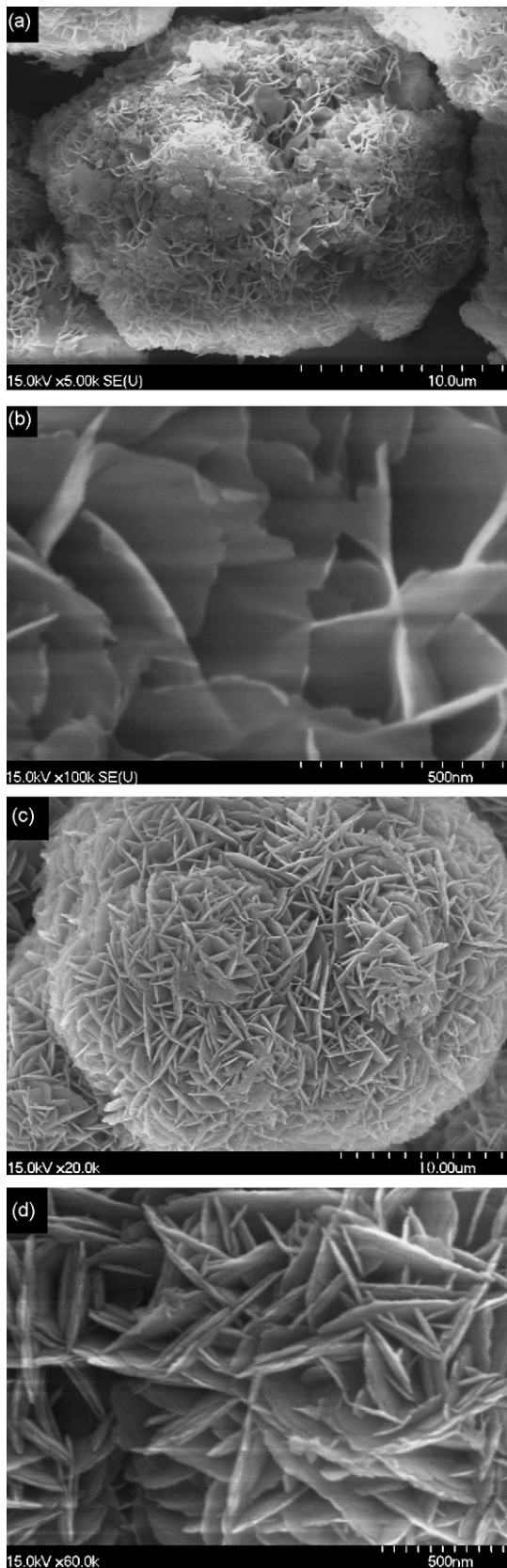


Fig. 2. SEM micrographs of the $\text{Ni}(\text{OH})_2$ samples: (a and b) $\text{Ni}(\text{OH})_2/\text{C}$ composite and (c and d) pure $\text{Ni}(\text{OH})_2$.

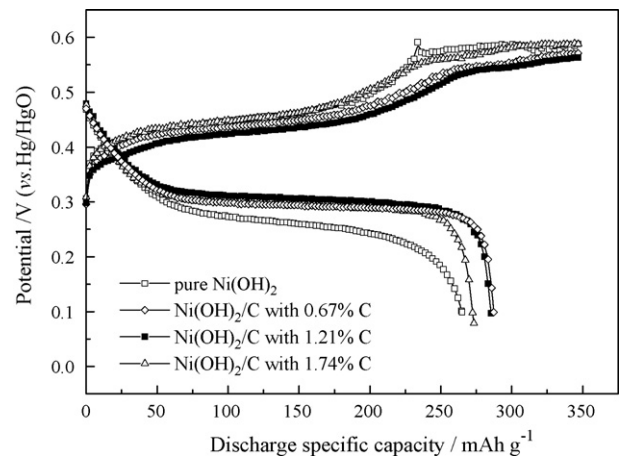


Fig. 3. Charge–discharge curves of the $\text{Ni}(\text{OH})_2/\text{C}$ samples with different carbon content at 1C-rate after activation.

Fig. 4 shows the cycling stability of two electrodes under different discharge rate conditions. During these cycle processes, the electrode with the $\text{Ni}(\text{OH})_2/\text{C}$ composite all shows higher specific capacity and better cycling stability than the electrode with pure $\text{Ni}(\text{OH})_2$. The capacity fading of the $\text{Ni}(\text{OH})_2/\text{C}$ composite at 5 and 10C discharge rates is restricted to a very lower level, even after long-term cycling, while that of pure $\text{Ni}(\text{OH})_2$ diminishes quickly. It indicates that the existence of carbon in the $\text{Ni}(\text{OH})_2/\text{C}$ composite enhances the cycling stability and extends the lifespan of the positive electrode at high-discharge rates.

Table 1 shows the comparison of discharge specific capacities of two electrodes. The discharge specific capacities are the average data of 100 charge–discharge cycles. The electrode with the $\text{Ni}(\text{OH})_2/\text{C}$ composite delivers a discharge capacity of 281 mAh g^{-1} , while the electrode with pure $\text{Ni}(\text{OH})_2$ delivers a discharge capacity of 247 mAh g^{-1} at 1C-rate. At 5C-rate, the discharge capacity of the $\text{Ni}(\text{OH})_2/\text{C}$ composite is 273 mAh g^{-1} , much higher than that of pure $\text{Ni}(\text{OH})_2$. And at 10C-rate, the discharge capacity of the $\text{Ni}(\text{OH})_2/\text{C}$ composite still remains as high as 250 mAh g^{-1} , but that of pure $\text{Ni}(\text{OH})_2$ decreases a lot, only about 66 mAh g^{-1} .

Fig. 5 presents the cyclic voltammograms of two electrodes obtained after 100 charge–discharge cycles at 5C-rate. The measurement was made at 100% discharge of depth (DOD). Near the reduction peak belonging to the $\beta\text{-Ni}(\text{OH})_2/\beta\text{-NiOOH}$, another reduction peak occurs in the electrode with pure $\text{Ni}(\text{OH})_2$, as shown in Fig. 4(b). According to the former research [4,22], the new-occurred peak belongs to the $\alpha\text{-Ni}(\text{OH})_2$ reduced from $\gamma\text{-NiOOH}$. For the electrode with the $\text{Ni}(\text{OH})_2/\text{C}$ composite, no typical peak contributed by $\gamma\text{-NiOOH}$ is found in Fig. 4(a). Prolonged overcharge of $\beta\text{-Ni}(\text{OH})_2$ in KOH and the ageing of $\beta\text{-NiOOH}$ favor the formation of $\gamma\text{-NiOOH}$, which leads to the pulverization of the electrode and decay of the capacity. Just as previously discussed, the $\text{Ni}(\text{OH})_2/\text{C}$ composite has more crystal defects, which can provide higher proton diffusion coefficient and ionic conductivity. On the other hand, the carbon black distributed in the $\text{Ni}(\text{OH})_2/\text{C}$ material reduces inner resistance of $\text{Ni}(\text{OH})_2$ particles due to its highly accessible

Table 1

The discharge specific capacities of two electrodes for 100 charge–discharge cycles

Discharge rate (C)	$\text{Ni}(\text{OH})_2/\text{C}$ (mAh g^{-1})	$\text{Ni}(\text{OH})_2$ (mAh g^{-1})
1	281	247
5	273	123
10	250	66

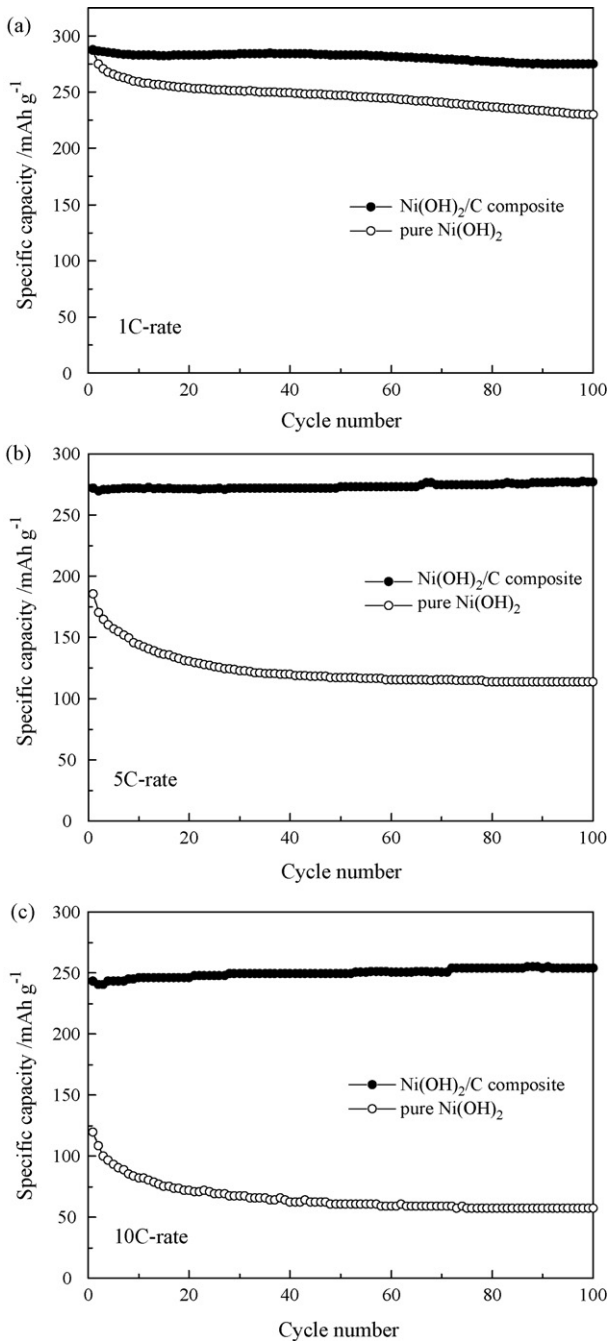


Fig. 4. Cycling stability of two electrodes under different discharge rate conditions.

surface and good electrical conductivity. All these factors help to diminish the polarization and amend the overcharge. So the formation of γ -NiOOH is restrained. Therefore, the electrode with the Ni(OH)₂/C composite will exhibit a stable discharge capacity and an extended lifespan.

Fig. 6 shows the typical charge–discharge profiles of two electrodes at the 50th cycle with 5C-rate. The electrode with the Ni(OH)₂/C composite presents much lower charge voltage plateau and higher discharge voltage plateau than the electrode with pure Ni(OH)₂, which indicates that the Ni(OH)₂/C composite has smaller polarization during the charge–discharge processes.

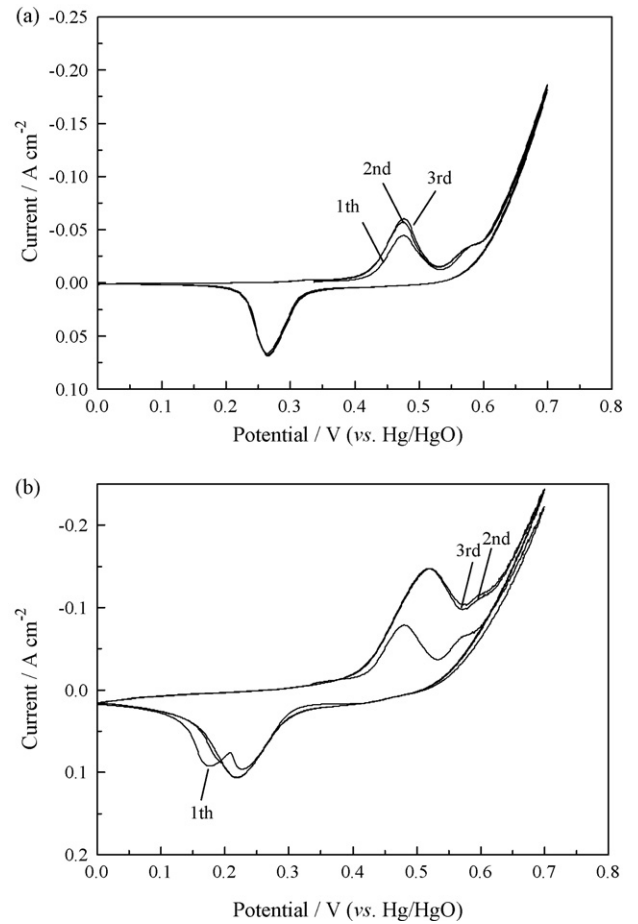


Fig. 5. Cyclic voltammograms with scan rate of 0.1 mV s^{-1} : (a) Ni(OH)₂/C composite, after 100 cycles at 100% DOD and (b) pure Ni(OH)₂, after 100 cycles at 100% DOD.

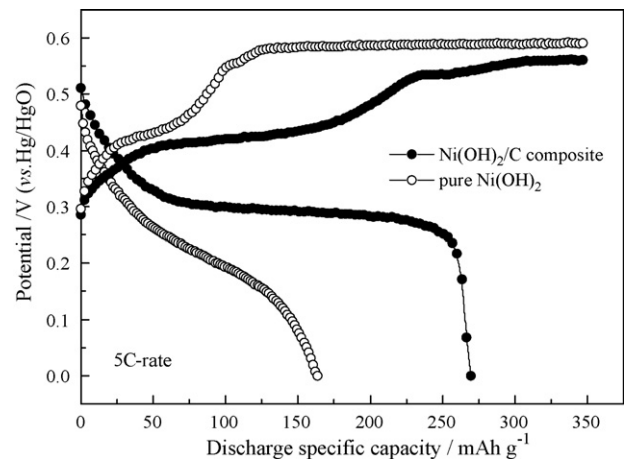


Fig. 6. Typical charge–discharge profiles of two electrodes at the 50th cycle with 5C-rate.

Table 2

The mean discharge voltages of two electrodes for 100 charge–discharge cycles

Electrode types	1 C-rate (V)	5 C-rate (V)	10 C-rate (V)
Ni(OH) ₂ /C	0.303	0.296	0.292
Ni(OH) ₂	0.266	0.231	0.227

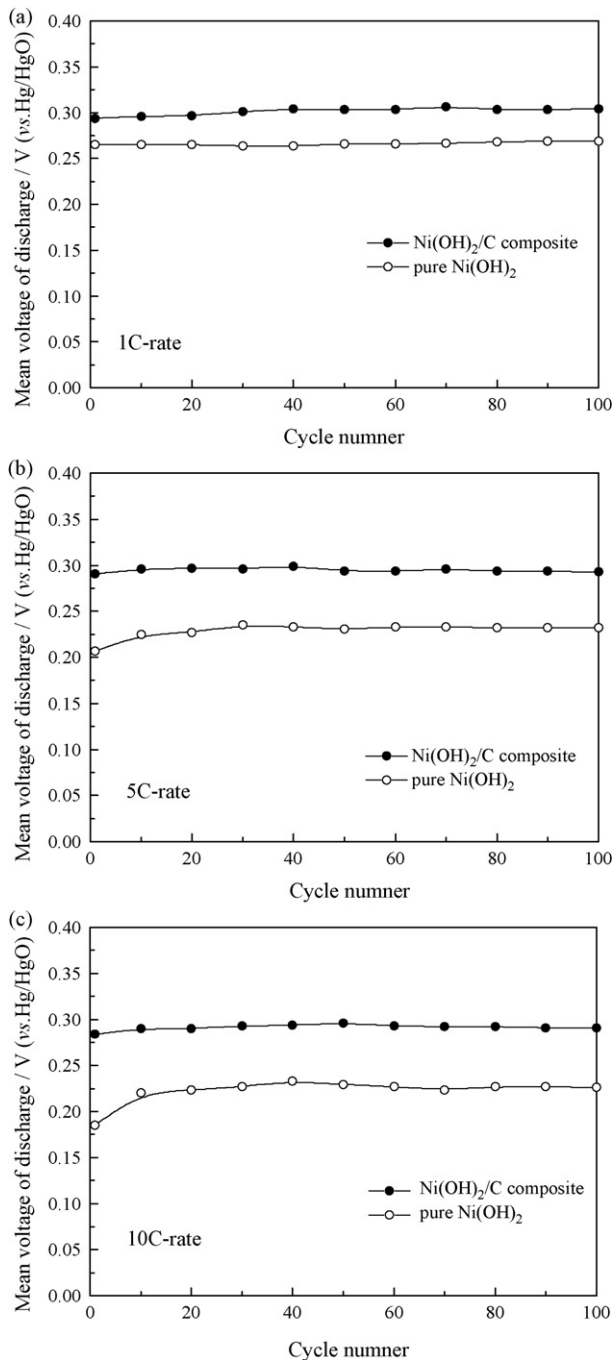


Fig. 7. Variation of mean discharge voltages of two electrodes with cycle number at different discharge rates.

3.3. Discharge potential analysis

The mean voltage of discharge is an important factor for Ni/MH rechargeable batteries. Higher mean voltage of discharge suggests more energy that the electrode can store and release. Table 2 shows the mean discharge voltages of two electrodes for 100 charge–discharge cycles at different discharge rates. It can be seen that the electrode with the Ni(OH)₂/C composite has much higher discharge voltage than the electrode with pure Ni(OH)₂. The mean discharge voltages of the Ni(OH)₂/C composite electrode are about 0.303 V (vs. Hg/HgO) at 1 C-rate, 0.296 V at 5 C-rate and 0.292 V

at 10 C-rate, while the mean discharge voltages of pure Ni(OH)₂ electrode are just about 0.266 V at 1 C-rate, 0.231 V at 5 C-rate and 0.227 V at 10 C-rate. Fig. 7 shows the variation of the mean voltage of two electrodes with cycle number at different discharge rates. Obviously, the Ni(OH)₂/C composite has higher mean voltage discharge than pure β-Ni(OH)₂, especially at high-discharge rate.

The load voltage of chemical power sources is attributed to total polarization, and the high-total polarization would lead to low load voltage. From the discussion above, the Ni(OH)₂/C composite not only prevents the formation of γ-NiOOH during high-rate charge–discharge cycling processes, but also helps to reduce the ohmic polarization and charge–transfer polarization. Therefore, the mean discharge voltage is optimized by the addition of carbon black, which is beneficial to electrochemical reversible reaction and the high-rate discharge performance of Ni(OH)₂ electrode.

4. Conclusion

The Ni(OH)₂/C composite has been synthesized by a simple co-precipitation method. In comparison with pure Ni(OH)₂, the as-synthesized Ni(OH)₂/C material has more crystal defects, and shows improved high-rate discharge performance, including superior cycling stability, higher discharge capacity and higher discharge potential. The discharge capacity and mean discharge voltage of the Ni(OH)₂/C composite are about 281 mAh g⁻¹ and 0.303 V (vs. Hg/HgO) at 1 C-rate, 273 mAh g⁻¹ and 0.296 V at 5 C-rate, 250 mAh g⁻¹ and 0.292 V at 10 C-rate. The cyclic voltammetry tests reveal that the Ni(OH)₂/C composite exhibits good electrochemical reversibility and the formation of γ-NiOOH during charge–discharge processes is prevented. The existence of carbon in the Ni(OH)₂/C composite contributes great effect on the improvement of high-rate discharge performance. Therefore, it is a promising positive material for high-power Ni/MH batteries.

Acknowledgement

This work was supported by the National Natural Science Foundation of China (No. 20673100).

References

- [1] D. Ohms, M. Kohlhasse, G. Benzúr-Urmössy, G. Schädlich, J. Power Sources 105 (2002) 127–133.
- [2] P. Oliva, J. Leonardi, J.F. Laurent, C. Delmas, J.J. Braconnier, M. Figlarz, F. Fievet, A. de Guibert, J. Power Sources 8 (1982) 229–255.
- [3] D.M. Constantin, E.M. Rus, L. Oniciu, L. Ghergari, J. Power Sources 74 (1998) 188–197.
- [4] M. Oshitani, H. Yufu, K. Takashima, S. Tsuji, Y. Matsumaru, J. Electrochem. Soc. 136 (1989) 1590–1593.
- [5] A.B. Yuan, S.A. Cheng, J.Q. Zhang, C.A. Cao, J. Power Sources 77 (1999) 178–182.
- [6] P. Elumalai, H.N. Vasan, N. Munichandraiah, J. Power Sources 93 (2001) 201–208.
- [7] X.Y. Wang, J. Yan, H.T. Yuan, Z. Zhou, D.Y. Song, Y.S. Zhang, L.Q. Zhu, J. Power Sources 72 (1998) 221–225.
- [8] W.K. Hu, X.P. Gao, M.M. Geng, Z.X. Gong, D. Noreus, J. Phys. Chem. B 109 (2005) 5392–5394.
- [9] A. Audemer, A. Delahaye, R. Farhi, N. Sac-Epée, J.M. Tarascon, J. Electrochem. Soc. 144 (1997) 2614–2620.
- [10] M. Oshitani, T. Takayama, K. Takashima, S. Tsuji, J. Appl. Electrochem. 16 (1986) 403–408.
- [11] A. Cressent, V. Pralong, A. Audemer, J.B. Leriche, A. Delahaye-Vidal, J.M. Tarascon, Solid State Sci. 3 (2001) 65–80.
- [12] J.H. Park, S. Kim, O.O. Park, J.M. Ko, Appl. Phys. A 82 (2006) 593–597.
- [13] A.H. Zimmerman, P.K. Effa, J. Electrochem. Soc. 131 (1984) 709–713.
- [14] D.A. Corrigan, R.M. Bendert, J. Electrochem. Soc. 136 (1989) 723–727.
- [15] C. Delacourt, C. Wurm, L. Laffont, J.B. Leriche, C. Masquelier, Solid State Ionics 177 (2006) 333–341.

- [16] X. He, J. Li, H. Chen, C. Jiang, C. Wan, J. Power Sources 152 (2005) 285–290.
- [17] J. Lv, J.P. Tu, W.K. Zhang, J.B. Wu, H.M. Wu, B. Zhang, J. Power Sources 132 (2004) 282–287.
- [18] C. Tessier, P.H. Haumesser, P. Bernard, C. Delmas, J. Electrochem. Soc. 146 (1999) 2059–2067.
- [19] S. Deabate, F. Fourgeot, F. Henn, J. Power Sources 87 (2000) 125–136.
- [20] R.S. Jayashree, P.V. Kamath, G.N. Subbanna, J. Electrochem. Soc. 147 (2000) 2029–2032.
- [21] K. Watanabe, T. Kikuoka, N. Kumagai, J. Appl. Electrochem. 25 (1995) 219–226.
- [22] R.D. Armstrong, H. Wang, Electrochim. Acta 36 (1991) 759–762.